# BooNE Has Begun

E. D. Zimmerman[a*]

[a]University of Colorado
Boulder, Colorado 80309



E898, the MiniBooNE experiment at Fermi National Accelerator Laboratory, has begun data collection. The experiment will test the neutrino oscillation signal reported by the Liquid Scintillator Neutrino Detector at Los Alamos National Laboratory. Data collection began in late August 2002.

## 1. PHYSICS INTRODUCTION: LSND and KARMEN

There are now several sources of evidence for neutrino oscillations. There is evidence from solar neutrino experiments, which observe fewer electron neutrinos than would be consistent with the sun's energy output [1]. In addition, the recent SNO results indicate that there is a non-electron flavor active neutrino component in the solar flux [2,3]. Evidence also comes from experiments studying neutrinos produced by cosmic rays in the earth's atmosphere, which find that muon neutrinos entering the detector from below (which had to travel through the earth) are depleted when compared with those incident from above (which traveled a shorter distance) [4]. Finally, there is evidence from a lone accelerator experiment, LSND at Los Alamos, which observed an excess of $\bar{\nu}_e$ events from a predominantly $\bar{\nu}_\mu$ source [5].

LSND used a beam-stop neutrino source at the 800 MeV LAMPF proton accelerator. The primary source of neutrinos was $\pi^+$ and $\mu^+$ decays at rest (DAR) in the target, which yielded $\nu_\mu$, $\bar{\nu}_\mu$, and $\nu_e$ with energies below 53 MeV. In addition, $\pi^+$ and $\pi^-$ decays in flight (DIF) provided a small flux of higher-energy $\nu_\mu$ and $\bar{\nu}_\mu$. The $\bar{\nu}_e$ flux was below $10^{-3}$ of the total DAR rate. The LSND data were collected between 1993 and 1998. The first data set, collected 1993-1995, used a water target and provided of 59% of the DAR flux; the remainder of the running used a heavy metal target composed mostly of tungsten. The collaboration searched for $\bar{\nu}_e$ appearance using the reaction $\bar{\nu}_e p \to e^+ n$ in a 167-ton scintillator-doped mineral oil ($CH_2$) target/detector. The detector sat 30 m from the target, providing an oscillation scale $L/E \sim 0.6 - 1$ m/MeV. The detector, which was instrumented with 1220 8-inch photomultiplier tubes (PMTs), observed a Čerenkov ring and scintillation light from the positron emitted in the neutrino interaction. An additional handle was the detection of the 2.2 MeV neutron-capture gamma ray from the reaction $np \to d\gamma$. The appropriate delayed coincidence (the neutron capture lifetime in oil is 186 $\mu$ s) and spatial correlation between the $e^+$ and $\gamma$ were studied for DAR $\bar{\nu}_e$ candidates.

In 2001, LSND presented the final oscillation search results, which gave a total $\bar{\nu}_e$ excess above background of $87.9 \pm 22.4 \pm 6.0$ events in the DAR energy range. The dominant background was beam-unrelated events, primarily from cosmic rays. These backgrounds were measured using the 94% of detector livetime when the beam was not on. No significant signal was observed in DIF events; the total $\nu_e/\bar{\nu}_e$ excess above background was $8.1 \pm 12.2 \pm 1.7$ events, consistent with the DAR result. The total events and energy distributions of the DAR and DIF events were used to constrain the oscillation parameter space (Fig. 1).

Another experiment of similar design, the Karlsruhe-Rutherford Medium Energy Neutrino (KARMEN) experiment at the ISIS facility of the Rutherford Laboratory, also searched for $\bar{\nu}_\mu \to \bar{\nu}_e$

*For the BooNE Collaboration.

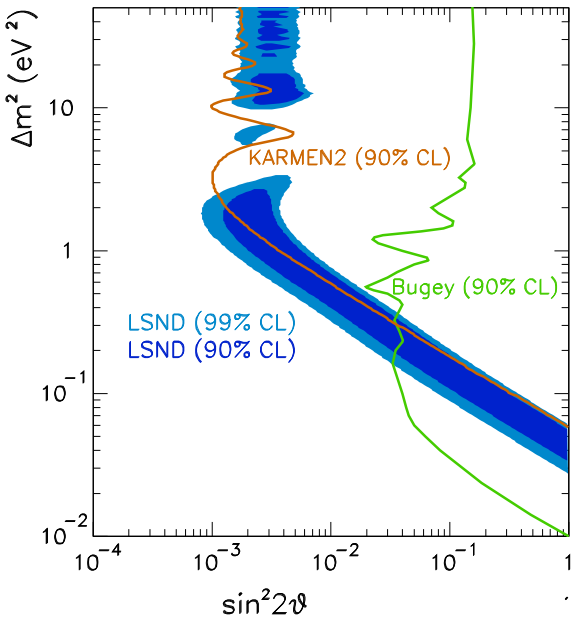


Figure 1. LSND 90% and 99% confidence level allowed regions (shaded) along with KARMEN2 and Bugey 90% confidence level exclusion limits and expected MiniBooNE sensitivity.

oscillations. KARMEN used a similar beam-stop neutrino source, but with a segmented smaller neutrino target (56 tons). KARMEN's sensitivity was enhanced because the lower beam duty factor ($10^{-5}$) allowed beam-unrelated events to be removed more effectively with a timing cut. In addition, KARMEN had higher flux because it was closer to the target (18 m versus 30 m). This did, however, reduce KARMEN's sensitivity to low-$\Delta m^2$ oscillations compared to LSND. KARMEN's most recent published result [7], using data collected from 1997 to 2001, reported 15 $\bar{\nu}_e$ oscillation candidates with an expected background of $15.8 \pm 0.5$ events. This result does not provide evidence for oscillations, and indeed can be used to rule out most of the high-$\Delta m^2$ portions of the LSND allowed region. However, an analysis of the combined LSND and KARMEN data sets has found regions of oscillation parameter space which fit both experiments' data well [8].

The LSND data indicate a much larger $\Delta m^2$ than atmospheric or solar experiments: $\Delta m^2 \sim 0.1 - 10$ eV$^2$. This led to the paradox of three $\Delta m^2$ values all of different orders of magnitude; this is impossible if there are only three neutrino masses. The more common way to account for all the existing oscillation data is to introduce one or more "sterile" neutrino flavors [9]. A more recent idea, motivated by extra-dimensions models, has been to introduce maximal $CPT$ violation in the neutrino mass matrix, thereby giving neutrinos and antineutrinos differing mass hierarchies [10].

## 2. MiniBooNE OVERVIEW

MiniBooNE (Experiment 898 at Fermilab) [6] is a short-baseline neutrino oscillation experiment which is designed to confirm or rule out LSND unequivocally. It uses an 8 GeV proton beam from the Fermilab Booster to produce pions, which are focused by a horn into a decay pipe, where they decay in flight to produce a nearly pure $\nu_\mu$ beam. The neutrinos are detected at a mineral oil Čerenkov detector 500 m away. The detector will use Čerenkov ring shape information to distinguish charged-current $\nu_\mu$ from $\nu_e$ interactions, searching for an excess of $\nu_e$ which would indicate oscillations. Data collection began in late summer 2002 and is expected to last two to three years. MiniBooNE is the first stage of the BooNE program, which will continue with a two-detector experiment to make precise measurements of oscillation parameters if LSND is confirmed.

There are several major differences between MiniBooNE and LSND, which should assure that systematic errors are independent. First, MiniBooNE operates at an energy and oscillation baseline over an order of magnitude greater than LSND: $E_\nu \sim 500 - 1000$ MeV, compared to $30 - 53$ MeV at LSND. The baseline $L = 500$ m, versus 30 m at LSND. $L/E$ remains similar, ensuring that the oscillation sensitivity is maximized in the same region of parameter space as LSND. MiniBooNE uses the quasielestic neutrino scattering reaction $\nu_e {}^{12}\mathrm{C} \rightarrow e^- X$ with the lead-

ing lepton's Čerenkov ring reconstructed, rather than LSND's antineutrino interaction with a hydrogen nucleus followed by neutron capture. Finally, MiniBooNE's goal is a factor of ten higher statistics than LSND had.

## 3. BEAM DETAILS

The BooNE neutrino beam begins with an 8 GeV primary proton beam from the Fermilab Booster accelerator. The beam arrives in 1.6 $\mu$s pulses, with five pulses per second. Within each pulse, the beam arrives in 80 bunches ("RF buckets") 19 ns apart. Protons from the primary beam strike a 71 cm beryllium target, producing short lived hadrons with a typical transverse momentum of 0.3 GeV/$c$. The hadrons are focused by the magnetic fields generated from a high-current-carrying device called a "horn." The target is located within the magnetic focusing horn. A horn was chosen because it gives higher angular and momentum acceptances than other focusing systems. It can be made to withstand high radiation levels, has cylindrical symmetry, and also gives sign selection.

A horn (see Fig. 2) contains a pulsed toroidal magnetic field in the volume between two coaxial conductors. Current flows along the inner (small radius) conductor and back along the outer (large radius) conductor. There is no field inside the inner conductor, nor outside the outer conductor. In the volume between the inner and outer conductors, the magnitude of the field is given by $B(\mathrm{kG}) \approx 0.2 \cdot I(\mathrm{kA})/R(\mathrm{cm})$, and its direction is azimuthal (the field lines are toroidal, encircling the inner conductor). The inner conductor shape and current were optimized by using GEANT [11] to maximize the $\nu_\mu$ flux between 0.5-1 GeV at the detector while minimizing flux above 1 GeV. The horn was optimized to run at 170 kA for $10^8$ pulses with $< 3\%$ fatigue failure probability.

Despite focusing, a highly divergent hadron beam exits the horn and enters the decay pipe. This beam consists mainly of unscattered and scattered primary protons and mesons. The decay pipe is 50 m long and six feet in diameter; most of the kaons and about a quarter of the pions decay before reaching its end. At the end of the decay pipe, 50 m from the target, is a beam absorber which stops all the hadrons and low-energy muons. Located 25 m from the target is an intermediate absorber which can be lowered into the beam. This design feature was introduced to provide a systematic check on muon-decay $\nu_e$ background.

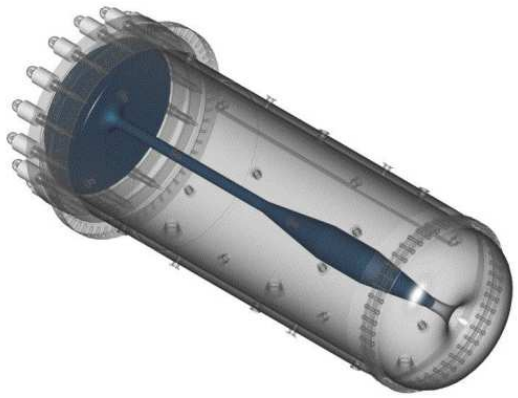

Figure 2. A view of the focusing horn. Beam enters from the upper left. All elements shown are aluminum. The outer conductor is rendered transparent. The target resides inside the narrow neck of the upstream end of the inner conductor. The inner conductor is six feet long, and the horn's diameter is two feet. *Image by Bartoszek Engineering.*

The neutrino flux which results from this design was simulated using GEANT with the standard FLUKA hadron interaction package. Efforts to simulate the flux using the MARS [12] simulation package are underway. All beamline elements, including the horn, shielding, and absorbers, were simulated. The $\nu_\mu$ flux at 500 m (in the absence of neutrino oscillations) for a detector on the $z$-axis with 6 m radius is shown as the solid histogram in Fig. 3. Using a Gaussian fit, the peak of the spectrum is at 0.94 GeV. Forty-eight percent of the spectrum is in the optimal range, between 0.3 and 1.0 GeV. The intrinsic $\nu_e$ background is shown as well; it results primarily from $K^+$, $K^0_L$, and $\mu^+$

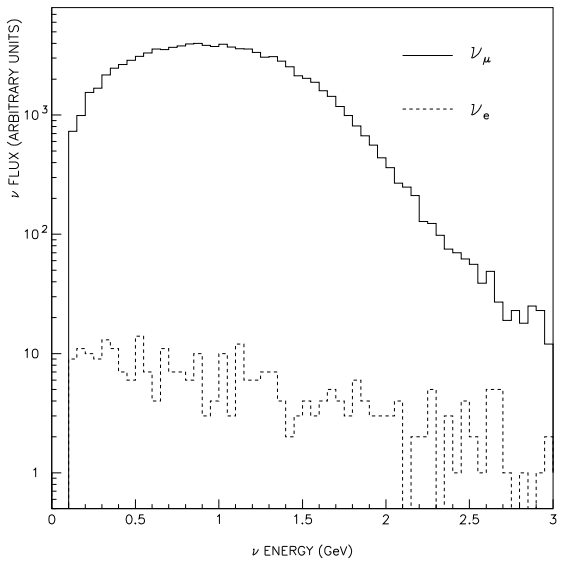


Figure 3. The $\nu_\mu$ flux (solid) at the MiniBooNE detector compared to the $\nu_e$ background (dashed).

decays.

## 4. DETECTOR DETAILS

The MiniBooNE detector is a 40-foot spherical tank filled with 800 tons of clear mineral oil and instrumented with 1520 8-inch PMTs. An optical barrier mounted 35 cm from the tank wall separates the inner fiducial region from an outer oil region which is used as a veto. The inner volume is lined with 1280 PMTs mounted directly on the optical barrier. The remaining 240 PMTs are mounted in the veto region. Most of the PMTs were acquired from LSND.

The detector records the hit arrival time and total charge for each PMT with $\geq 1$ photoelectron in each 100 ns clock cycle. From the PMT information, Čerenkov rings and delayed scintillation light are reconstructed. The oil was not doped with scintillator; the natural scintillation properties of mineral oil are near optimal for the experiment.

The Čerenkov ring allows the track direction and location to be calculated, as well as providing the primary means of particle identification. Electrons are identified by their characteristic ring shape, a result of the electromagnetic shower profile. Muons have a ring shape characteristic of a penetrating track with little scattering: the outer edge of the ring is well-defined and the ring is significantly filled in due to the extended track. Muons are further identified by their decay electron, except for the 8% of $\mu^-$ which are captured by nuclei. Finally, a source of potential background to the $\nu_e$ signal is neutral-current production of nucleon resonances which decay to $\pi^0$. The $\pi^0 \rightarrow \gamma\gamma$ decay produces two electromagnetic showers, each one of which appears very similar to an electron ring. In asymmetric decays, one ring may not be reconstructed. The recoil nucleon from the resonance decay, while usually below Čerenkov threshold, produces additional scintillation light which can help distinguish $\pi^0$ events from $\nu_e$. In the end, the $\pi^0$ misidentification background is expected to be comparable to or below an anticipated oscillation signal. Muon misidentification levels should be lower yet.

## 5. STATUS AND CONCLUSION

MiniBooNE began taking neutrino physics data in August 2002. As of early November, several thousand neutrino events have been recorded. A blind analysis is being performed, removing $\nu_e$ candidates from the samples which are open to study. An early $\nu_\mu$ candidate event display is shown in Fig. 4.

The beam and detector were commissioned quickly, and within a few weeks of the first neutrino data protons were being delivered reliably at a rate of $10^{16}$ per hour. This is, however, a factor of eight below the nominal intensity. The Booster's ability to deliver beam is at present limited by radiation losses in the accelerator and extraction system. Work is ongoing to improve this rate, and with luck the Booster will be delivering nearly the full requested intensity to MiniBooNE by early in the next calendar year. This will allow MiniBooNE to publish results addressing LSND

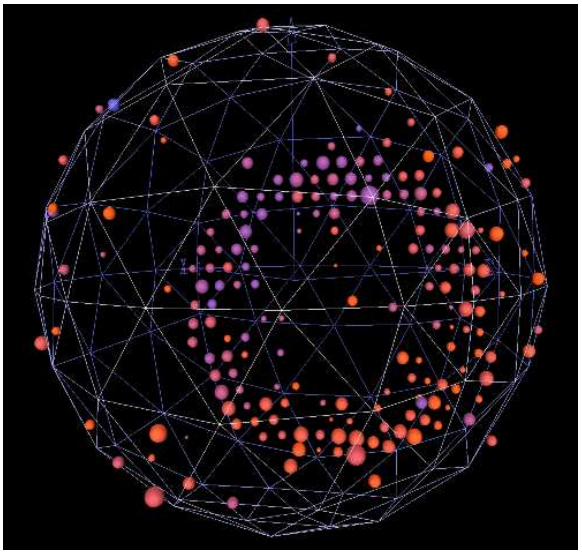

Figure 4. Neutrino event from first running period. The colors indicate hit timing; the size of the colored blobs indicates the total charge on each PMT.

in two years.

## REFERENCES


1. Y. Fukuda *et al.*, *Phys. Rev. Lett.* **82** 2430 (1999).
   J.N. Abdurashitov *et al.*, *Phys. Rev. Lett.* **83** 4686 (1999).
   GALLEX Collab., *Phys. Lett.* **B447** 127 (1999).
2. SNO Collab., Q.R. Ahmad *et al.*, nucl-ex/0106015
3. Q. R. Ahmad *et al.*, nucl-ex/0204008
4. Y. Fukuda *et al.*, *Phys. Rev. Lett.* **81** 1562 (1998).
   M. Ambrosio *et al.*, Phys. Lett. **B 478** 5 (2000).
   W.A. Mann, Proceedings of Neutrino 2000, *Nucl. Phys. B (Proc. Suppl.)* **91** 134 (2001).
5. A. Aguilar *et al.*, *Phys. Rev.* **D64** 112007 (2001).
6. The MiniBooNE web site, found at `http://www-boone.fnal.gov`, offers information about the experiment.
7. B. Armbruster *et al.*, *Phys. Rev.* **D65** (2002).
8. E. Church *et al.*, *Phys. Rev.* **D66** 013001 (2002).
9. V. Barger *et al.*. *Phys. Lett.* **B489** 345 (2000).
10. G. Barenboim *et al.*, *J. High Energy Phys.* **0210** 001 (2002).
11. Applications and Software Group, CERN, Program Library Report Q123.
12. `http://www-ap.fnal.gov/MARS`.